

Analysis of Rayleigh surface wave propagation in isotropic micropolar solid under three-phase-lag model of thermoelasticity

Soumen Shaw* and Basudeb Mukhopadhyay

Department of Mathematics, IEST, Shibpur, India

The present paper is dealing about the Rayleigh surface wave propagation in an isotropic-micropolar-thermoelastic solid by employing the three-phase-lag thermoelasticity theory. The secular equations for insulated as well as isothermal boundary conditions are derived analytically. Effect of phase lags on phase velocity, attenuation coefficient and specific loss factor are illustrated in different figures and the salient features are emphasised.

Keywords: Rayleigh surface wave; three-phase lag; micropolar thermoelasticity; phase velocity; attenuation coefficient; specific loss

1. Introduction

In recent years there has been very much written on the subject of the theory of elastic solids in which the deformation is described not only by the usual vector displacement field but also by other vector or tensor fields. In a series of papers, Eringen (1964, 1967), Eringen and Kafadar (1976) and Eringen and Suhubi (1964) established the general theory of micromorphic continua to predict the behaviour of materials with inner structure. Later on, the microstretch and micropolar elasticity are also introduced by Eringen (1966, 1971). The material points of microstructure solids can stretch and contract independently of their translations and rotations. In general, the microstretch continua are used to characterise composite materials and various porous media. Including heat conduction, Eringen (1999) extended the micropolar theory to micropolar thermoelasticity. A generalised theory of linear micropolar thermoelasticity that admits the possibility of “second sound” effects has been established by Boschi and Ieşan (1973). Dost and Tabarrok (1978) presented the generalised micropolar thermoelasticity by using Green–Lindsay theory.

In modern technology, high-rate heating is a rapidly emerging area in heat transfer. In this case, the non-equilibrium thermodynamic transition, shortening the response time and microscopic effects in the energy exchange are the two important issues to be faced. In the microscopic two-step model of laser heating, the temperature of the metal lattice may remain undisturbed, while the energy exchange between phonons and free electrons is taking place. Relative to the time at which the electron gas starts to receive the phonon energy from the laser source, therefore, increase in the lattice temperature is delayed due to phonon–electron interactions on the microscopic level. Hence, a microscopic level time lag is possible in between the temperature gradient, heat flux vector and thermal displacement.

*Corresponding author. Email: shaw_soumen@rediffmail.com

Since last one decade, many researchers are devoted themselves in the characteristic analysis of phase lags. Some heat conduction problems on phase lags and its stability analysis were discussed by Quintanilla (2009, 2011) and Quintanilla and Racke (2008). Tzou, (1995a, 1995b, 1995c, 1997) discussed different aspects of phase lagging in heat conduction. Roy Choudhuri (2007a, 2007b) extended the dual-phase-lag model incorporating three-phase-lag concept. Several researchers have attempted to investigate the propagation of plane harmonic wave in elastic media. By employing phase-lag concepts, the propagation of plane waves have discussed by Mukhopadhyay and Kumar (2010) and Kanoria and Mallik (2010). Rayleigh wave propagation in thermoelastic half-space using dual-phase-lag model was investigated by Abouelregal (2011).

The present paper is an investigation on Rayleigh surface waves in a homogeneous-isotropic-micropolar elastic solid. In this context, heat conduction equation with three-phase lags has been considered. Various aspects of this wave propagation are discussed in the section of numerical analysis and observations and the effects of phase lags are also pointed out.

2. Basic equations

It is important to remember that the model proposed by Tzou (1995a) contains the theories of Lord–Shulman (Lord & Shulman, 1967), Green–Lindsay (Green & Lindsay, 1972) as particular cases. When several orders of approximation are considered in Tzou’s theory, the classical theory of Cattaneo (1948) is obtained. However, the theories proposed by Green–Naghdi (Green & Naghdi, 1991, 1992, 1993) cannot be obtained from that point of view. Recently, Roy Choudhuri (2007a) has proposed a theory with three-phase lag which is able to contain all the previous theories at the same time. The basic equation is

$$\vec{q}(\vec{r}, t + \tau_q) = -(k\nabla T(\vec{r}, t + \tau_T) + k^*\nabla v(\vec{r}, t + \tau_v)) \quad (2.1)$$

Here, \vec{q} is the heat flux vector, T is the temperature and v is the thermal displacement that satisfies $\dot{v} = T$. τ_T , τ_q , τ_v are the phase lags of the temperature gradient, heat flux and temperature displacement, respectively. k is the thermal conductivity and k^* represents the conductivity rate.

By Taylor Series expansion of the Equation (2.1), we obtain

$$\vec{q}(\vec{r}, t) + \tau_q \frac{\partial \vec{q}}{\partial t}(\vec{r}, t) + \frac{1}{2} \tau_q^2 \frac{\partial^2 \vec{q}}{\partial t^2}(\vec{r}, t) = -k \left[\nabla T(\vec{r}, t) + \tau_T \frac{\partial}{\partial t}(\nabla T(\vec{r}, t)) \right] - k^* \left[\nabla v(\vec{r}, t) + \tau_v \frac{\partial}{\partial t}(\nabla v(\vec{r}, t)) \right] \quad (2.2)$$

$$\text{Energy equation: } -\nabla \cdot \vec{q}(\vec{r}, t) = \rho C_e \dot{T}(\vec{r}, t) + T_0 \beta_0 \dot{\varepsilon}_{kk}(\vec{r}, t), \quad (2.3)$$

where C_e is the specific heat at constant strain, T_0 is the reference temperature, ρ is density of the material, $\beta_0 = (3\lambda + 2\mu + \kappa)\alpha_t$, α_t is the coefficient of linear thermal expansion and ε_{ij} is the micropolar strain tensor. Overheaded dot denotes the time derivatives.

Coleman, Fabrizio, and Owen (1982, 1986) proved that the internal energy must contain a term proportional to the squared of heat flux for a pure wave’s behaviour to exist in heat conduction equation. Equation (2.3) does not incorporate this feature due to the mixed behaviour of waves (represented by τ_q) and the microstructural effect (τ_T). However, heat flux dependent internal energy into the energy equation does not violate the solutions much (Bai & Lavine, 1992).

Combining Equations (2.2) and (2.3), we obtain

$$\left(k^* + \left(\tau_v^* + k\tau_T \frac{\partial}{\partial t}\right) \frac{\partial}{\partial t}\right) \nabla^2 T = \left(1 + \tau_q \frac{\partial}{\partial t} + \frac{1}{2} \tau_q^2 \frac{\partial^2}{\partial t^2}\right) (\rho C_e \ddot{T} + T_0 \beta_0 \ddot{\epsilon}_{kk}) \quad (2.4)$$

where $\tau_v^* = k^* \tau_v + k$.

Though the time lags τ_q, τ_v are very small, the inequality $\tau_v^* > \tau_q k^*$ is not always true; thus, for the stability of solutions of the considered Equation (2.4) (Quintanilla & Racke, 2008) here, we have taken up to second degree terms of τ_q in Taylor Series expansion of the heat flux vector term.

Particular cases:

(1) when $k^* = 0$, Equation (2.4) reduces to

$$k \left(1 + \tau_T \frac{\partial}{\partial t}\right) \nabla^2 T = \left(1 + \tau_q \frac{\partial}{\partial t} + \frac{1}{2} \tau_q^2 \frac{\partial^2}{\partial t^2}\right) (\rho C_e \dot{T} + T_0 \beta_0 \dot{\epsilon}_{kk})$$

This is the heat conduction equation in the context of thermoelasticity with dual-phase lags (Tzou 1995a).

(2) when $\tau_q = \tau_T = \tau_v = 0$, Equation (2.4) becomes

$$\left(k^* + k \frac{\partial}{\partial t}\right) \nabla^2 T = \rho C_e \ddot{T} + T_0 \beta_0 \ddot{\epsilon}_{kk},$$

which is the heat conduction equation of type GN-III (Green & Naghdi, 1993).

(3) when $k^* = \tau_T = \tau_v = 0$, $\tau_q = t_0$, $\tau_q^2 = 0$, from the Equation (2.4), we obtain

$$k \nabla^2 T = \left(1 + t_0 \frac{\partial}{\partial t}\right) [\rho C_e \dot{T} + T_0 \beta_0 \dot{\epsilon}_{kk}].$$

This is the thermoelastic heat conduction equation due to Lord and Shulman (1967).

3. Formulation of the problem

We consider a homogeneous-isotropic-thermally conducting micropolar elastic solid half-space initially undisturbed and at uniform temperature T_0 . We take origin of the coordinate system (x, y, z) on top surface of the solid half-space. The y -axis is taken pointing vertically downwards into the semi-space which is represented by $y \geq 0$. The x -axis is taken along the direction of the wave propagation, so all the particles on z -axis are equally displaced and hence all the field quantities are independent of z -coordinate. Further, it is assumed that the disturbances are small and are confined to the neighbourhood of the interface $y = 0$ and hence vanish as $y \rightarrow \infty$ (see Figure 1). The surface of the half-space is assumed to be free from force stresses and couple stresses and in addition, it is maintained at thermally insulated or isothermal conditions. The basic

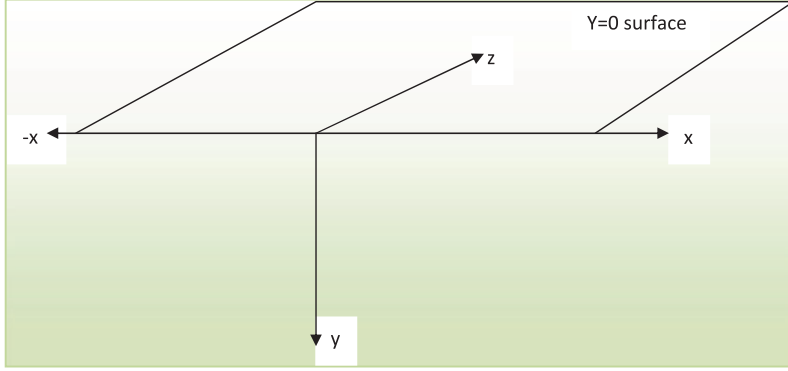


Figure 1. Geometry of the problem.

governing equations of motion and heat conduction to be specified by the displacement $\vec{u}(x, y, t)$, temperature change $T(x, y, t)$ and microrotation $\vec{\varphi}(x, y, t)$ are:

$$(\lambda + 2\mu + \kappa)\nabla \cdot (\nabla \cdot \vec{u}) - (\mu + \kappa)\nabla \times (\nabla \times \vec{u}) + \kappa(\nabla \times \vec{\varphi}) - \beta_0\nabla T = \rho \ddot{\vec{u}} \quad (3.1)$$

$$(\alpha + \beta + \gamma)\nabla \cdot (\nabla \cdot \vec{\varphi}) - \gamma\nabla \times (\nabla \times \vec{\varphi}) + \kappa(\nabla \times \vec{u}) - 2\kappa\vec{\varphi} = \rho j \ddot{\vec{\varphi}} \quad (3.2)$$

$$\left(k^* + \left(\tau_v^* + k\tau_T \frac{\partial}{\partial t} \right) \frac{\partial}{\partial t} \right) \nabla^2 T = \left(1 + \tau_q \frac{\partial}{\partial t} + \frac{1}{2} \tau_q^2 \frac{\partial^2}{\partial t^2} \right) (\rho C_e \ddot{T} + T_0 \beta_0 \ddot{\epsilon}_{kk}) \quad (3.3)$$

where $\alpha, \beta, \gamma, \kappa$ are elastic constants, λ, μ are Lamé's constants and j is the microinertia.

Now, we define the following dimensionless variables:

$$\begin{aligned} x' &= \frac{\omega^*}{c_1} x, \quad y' = \frac{\omega^*}{c_1} y, \quad u'_i = \frac{\omega^* \rho c_1}{\beta_0 T_0} u_i, \quad \varphi'_i = \frac{\kappa}{\beta_0 T_0} \varphi_i, \quad T' = \frac{T}{T_0}, \quad t' = \omega^* t, \quad \left\{ \tau'_T, \tau'_q, \tau'_v \right\} \\ &= \omega^* \left\{ \tau_T, \tau_q, \tau_v \right\}, \quad \delta^2 = \frac{c_2^2}{c_1^2}, \quad \delta_1^2 = \frac{\gamma}{\rho j}, \quad \delta_2^2 = \frac{\kappa^2}{\rho^2 j \omega^{*2}}, \quad \delta_3^2 = \frac{2\kappa c_1^2}{\rho j \omega^{*2}}. \end{aligned} \quad (3.4)$$

Here ω^* is characteristic frequency, c_1 is the longitudinal velocity, c_2 is the shear velocity.

Upon using the quantities given by (3.4) in the Equations (3.1)–(3.3), in the case of two-dimensional motions in xy plane, we obtain

$$u_{1,11} + (1 - \delta^2) u_{2,12} + \delta^2 u_{1,22} + \varphi_{,2} - T_{,1} = \ddot{u}_1 \quad (3.5)$$

$$\delta^2 u_{2,11} + (1 - \delta^2) u_{1,12} + u_{2,22} - \varphi_{,1} - T_{,2} = \ddot{u}_2 \quad (3.6)$$

$$\delta_1^2 \nabla^2 \varphi + \delta_2^2 (u_{2,1} - u_{1,2}) - \delta_3^2 \varphi = \ddot{\varphi} \quad (3.7)$$

$$\left[k_1 + \left(\tau_v^* + \omega^* \tau_T \frac{\partial}{\partial t} \right) \frac{\partial}{\partial t} \right] \nabla^2 T = \left(1 + \tau_q \frac{\partial}{\partial t} + \frac{\tau_q^2}{2} \frac{\partial^2}{\partial t^2} \right) [\ddot{T} + \epsilon \ddot{u}_{i,i}] \quad (3.8)$$

where $k_1 = \frac{k^*}{\rho C_e c_1^2}$, $\tau_v^* = k_1 \tau_v' + 1$, $\omega^* = \frac{\rho C_e c_1^2}{k}$, $\varepsilon = \frac{\beta_0^2 T_0}{\rho^2 c_1^2 C_e}$, and $\vec{u} = (u_1, u_2, 0)$, $\vec{\varphi} = (0, 0, \varphi)$.

4. Boundary conditions

The boundary conditions on the surface $y = 0$ of the solid half-space are given below:

Mechanical conditions: the surface of the solid is free from force stresses and couple stresses, i.e.

$$t_{21} = 0 = t_{22}, \quad m_{23} = 0 \quad \text{on } y = 0, \quad (4.1)$$

where $t_{21} = \delta^2 u_{1,2} + \frac{\mu}{\rho c_1^2} u_{2,1} + \varphi$ and $t_{22} = u_{2,2} + \frac{\lambda}{\rho c_1^2} u_{1,1} - T$.

Thermal conditions: the boundary of the half-space is thermally insulated or isothermal as

$$T_{,2} = 0 \quad \text{or} \quad T = 0, \quad \text{respectively.} \quad (4.2)$$

5. Solution of the problem

In order to solve the Equations (3.5)–(3.8), we introduce two potential functions $\psi_1, \vec{\psi}_2$ in the solid defined by,

$$\vec{u} = \text{grad}\psi_1 + \text{curl}\vec{\psi}_2, \quad \vec{\psi}_2 = \psi_2 \hat{e}_3 \quad (5.1)$$

where $\psi_1, \vec{\psi}_2$ are the velocity potential functions of longitudinal and shear waves in the solid, \hat{e}_3 is the unit vector along z -axis and hence (3.5)–(3.8) reduces to

$$\left(\nabla^2 - \frac{\partial^2}{\partial t^2} \right) \psi_1 - T = 0 \quad (5.2)$$

$$\left(\delta^2 \nabla^2 - \frac{\partial^2}{\partial t^2} \right) \psi_2 + \varphi = 0 \quad (5.3)$$

$$\left(\delta_1^2 \nabla^2 - \delta_3^2 - \frac{\partial^2}{\partial t^2} \right) \varphi - \delta_2^2 \nabla^2 \psi_2 = 0 \quad (5.4)$$

$$\left(k_1 + \left(\tau_v^* + \omega^* \tau_T \frac{\partial}{\partial t} \right) \frac{\partial}{\partial t} \right) \nabla^2 T = \left(1 + \tau_q \frac{\partial}{\partial t} + \frac{\tau_q^2}{2} \frac{\partial^2}{\partial t^2} \right) \left[\ddot{T} + \varepsilon \nabla^2 \ddot{\psi}_1 \right]. \quad (5.5)$$

We assume the solutions of the Equations (5.2)–(5.5) are of the form:

$$\{\psi_1, \psi_2, \varphi, T\} = \{\psi_1(y), \psi_2(y), \varphi(y), T(y)\} \exp\{i\xi(x - ct)\} \quad (5.6)$$

where $c = \frac{\omega}{\xi}$ is the phase velocity, ω is the circular frequency and ξ is wave number.

Upon using the Equation (5.6) into the Equations (5.2)–(5.5), we obtain

$$\{\psi_1, T\} = \sum_{k=1}^2 \{1, V_k\} (A_k \exp(m_k y) + B_k \exp(-m_k y)) \exp\{i\xi(x - ct)\}, \quad (5.7)$$

$$\{\psi_2, \varphi\} = \sum_{k=3}^4 \{1, S_k\} (A_k \exp(m_k y) + B_k \exp(-m_k y)) \exp\{i\xi(x - ct)\}, \quad (5.8)$$

where $V_k = \omega^2 (a_k^2 + 1)$, $S_k = \delta^2 (\beta^2 - m_k^2)$, $m_k^2 = \xi^2 (1 - a_k^2 c^2)$, $\beta^2 = \xi^2 \left(1 - \frac{c^2}{\delta^2}\right)$,

$$a_{1,2}^2 = \frac{\left[(1+\varepsilon) \left(i\omega^{-1} \tau_1 + \frac{\tau_2^*}{2} \right) - (k_1 \omega^{-2} - \tau_2) \right] \pm \sqrt{\left[(1+\varepsilon) \left(i\omega^{-1} \tau_1 + \frac{\tau_2^*}{2} \right) - (k_1 \omega^{-2} - \tau_2) \right]^2 - 4(k_1 \omega^{-2} - \tau_2) \left(i\omega^{-1} \tau_1 + \frac{\tau_2^*}{2} \right)}}{2(k_1 \omega^{-2} - \tau_2)},$$

$$a_{3,4}^2 = \frac{1}{2} \left[\frac{\delta^2 (\delta_3^2 - 1) - \delta_2^2 - \delta_1^2}{\omega^2} \pm \sqrt{\left(\frac{\delta^2 (\delta_3^2 - 1) - \delta_2^2 - \delta_1^2}{\omega^2} \right)^2 - 4 \left(1 - \frac{\delta_3^2}{\omega^2} \right)} \right], \quad \tau_1 = \tau_q + i\omega^{-1}, \tau_2 =$$

$$\omega^* \tau_T + i\omega^{-1} \tau_v^*.$$

These solutions constitute of pairs of partial waves propagating in both the directions along x -axis with the unknown amplitudes A_k and B_k , $k = 1, 2, 3, 4$. These forms of formal solution are appropriate for the description of wave propagation in an infinite thermoelastic micropolar media. Here, we are primarily interested in surface wave propagation along the free surface of the thermoelastic-micropolar-semi-space, so we choose the partial waves that satisfy radiation condition. Thus, for the wave propagation in generalised thermoelastic-micropolar half-space $y \geq 0$, we choose formal solutions satisfying the conditions $\text{Re}(m_k) \geq 0$, $k = 1, 2, 3, 4$ as:

$$\{\psi_1, T\} = \sum_{k=1}^2 \{1, V_k\} B_k \exp(-m_k y) \exp\{i\xi(x - ct)\}, \quad (5.9)$$

$$\{\psi_2, \varphi\} = \sum_{k=3}^4 \{1, S_k\} B_k \exp(-m_k y) \exp\{i\xi(x - ct)\}. \quad (5.10)$$

6. Dispersion equations

This section is devoted to the derivation of secular equations of Rayleigh surface waves in the considered media under different situations. Upon invoking the boundary conditions (4.1)–(4.2), we obtain a system of four algebraic equations with four unknowns B_k ($k = 1, 2, 3, 4$) for thermally insulated or isothermal half-space. For non-trivial solutions, equating the coefficient determinant with zero, which leads the governing equations of Rayleigh surface waves propagating in the considered media, we obtain

$$\begin{aligned} & \xi^2 \left(c^2 - \frac{2\mu + \kappa}{\rho c_1^2} \right)^2 (m_2 V_2 - m_1 V_1) (m_4 S_4 - m_3 S_3) \\ & + \left(\frac{2\mu + \kappa}{\rho c_1^2} \right)^2 m_1 m_2 m_3 m_4 (V_2 - V_1) (S_4 - S_3) = 0 \end{aligned} \quad (6.1)$$

This is the secular equation for thermally insulated boundary and

$$\begin{aligned} & \xi^2 \left(c^2 - \frac{2\mu + \kappa}{\rho c_1^2} \right)^2 (V_2 - V_1) (m_4 S_4 - m_3 S_3) \\ & + \left(\frac{2\mu + \kappa}{\rho c_1^2} \right)^2 m_3 m_4 (m_1 V_2 - m_2 V_1) (S_4 - S_3) \\ & = 0, \end{aligned} \quad (6.2)$$

represents the secular equation for isothermal boundary.

7. Solutions of dispersion equations

- (1) In general, wave number (ξ) and hence the phase velocity (c) of the wave are complex quantities, so that

$$\frac{1}{c} = \frac{1}{V} + i\frac{Q}{\omega},$$

where $\xi = R + iQ$, $R = \frac{\omega}{V}$, in which V and Q are real. The exponent term in the plane wave solution (5.6) is reduced to $iR(x - Vt) - Q(x - Vt)$. This shows that V is the propagation speed and Q is the attenuation coefficient of the wave.

- (2) The specific loss is the energy dissipated in taking a specimen through a stress cycle, ΔW , to the elastic energy stored in the specimen when the elastic energy is maximum, W . The specific loss is the most direct method of defining internal friction for material, (Puri & Cowin, 1985). For a sinusoidal plane wave of small amplitude, Kolsky (1963) prove that the specific loss $\frac{\Delta W}{W}$ equals to 4π times the absolute value of the imaginary part of ξ to the real part of ξ , i.e.

$$\frac{\Delta W}{W} = 4\pi \frac{|\text{Im}(\xi)|}{|\text{Re}(\xi)|} = 4\pi \left| \frac{VQ}{\omega} \right|,$$

where ξ is the complex number such that $\text{Im}(\xi) > 0$.

8. Numerical results and observations

In order to illustrate and verify the analytical results obtained in the previous sections, we present some numerical simulation results. The material chosen for this purpose is magnesium crystal whose data value is given below (Dhaliwal & Singh, 1980; Eringen, 1984).

- (1) Micropolar parameters:

$$\lambda = 9.4 \times 10^{10} \text{ Nm}^{-2}, \mu = 4.0 \times 10^{10} \text{ Nm}^{-2}, \kappa = 1.0 \times 10^{10} \text{ Nm}^{-2}, \rho = 1.74 \times 10^3 \text{ kg m}^{-3}, \gamma = .779 \times 10^{-9} \text{ N}, j = .2 \times 10^{-19} \text{ m}^2,$$

- (2) Thermal parameters:

$$K = 1.7 \times 10^2 \text{ J sec}^{-1} \text{ m}^{-1} \text{ deg}^{-1}, C_e = 1.04 \times 10^3 \text{ J kg}^{-1} \text{ deg}^{-1}, T = 298 \text{ K}.$$

Here we choose $k_1 = 1$.

The non-dimensional phase velocity, attenuation coefficient and specific loss factor for different values of time lags τ_q, τ_v, τ_T in the context of three-phase-lag, dual-phase-lag, Green–Naghdi (GN) and Lord–Shulman theories of thermoelasticity have been computed for various values of non-dimensional frequency from the secular Equations (6.1) and (6.2) for stress-free thermally insulated or isothermal boundaries.

In general, we know $c = \frac{\omega}{\zeta}$, where $\zeta = R + iQ$, $R = \frac{\omega}{V}$ in which V and Q are real. V is the propagation speed and Q is the attenuation coefficient of the wave. Therefore, for fixed value of ω , Equations (6.1) and (6.2) reduce to a function of ζ , i.e. $g(\zeta)$ say, then to obtain the solution apply fixed point iteration method on the equation $g(\zeta) = 0$ up to a desire level of accuracy. The results are presented graphically for thermally insulated and isothermal boundary conditions as function of frequency.

From Figures 2a, 2b and 3, it is noticed that the phase velocity for thermally insulated and isothermal boundaries remains almost identical for three-phase-lag, dual-phase-lag, GN-III and LS model. This quantity varies monotonically with increasing frequency. From Figure 2a, it seems that in the region $0 \leq \omega \leq 100$,

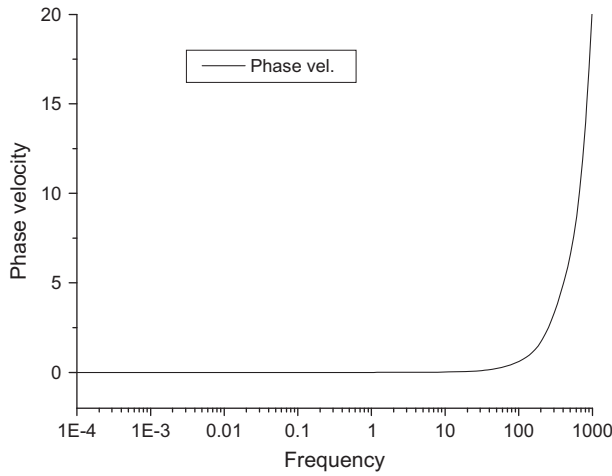


Figure 2a. Variation of phase velocity w.r.t. frequency.

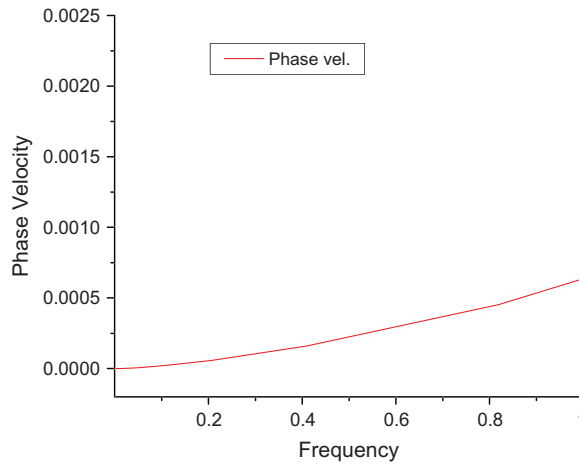


Figure 2b. Variation of phase velocity w.r.t. frequency (for small values of ω).

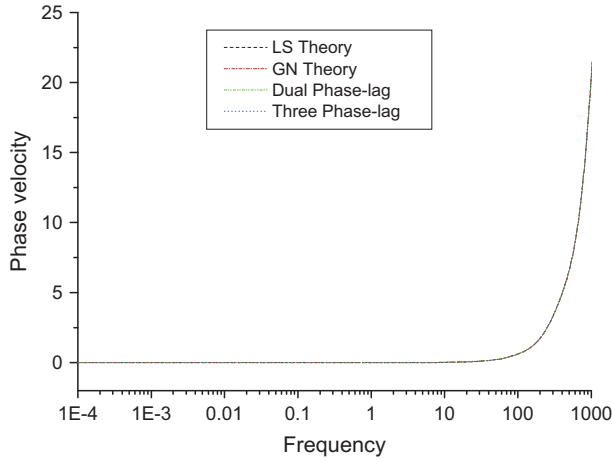


Figure 3. Variation of phase velocity w.r.t. frequency (for various thermoelastic models).

phase velocity is very close to zero and then in between $\omega = 100$ and 1000, phase velocity attains a very large value. But from Figure 2b, it is observed that the phase velocity is increasing very slowly with increasing frequency in the region $0 \leq \omega \leq 1$. That means the value of the phase velocity increases with increasing value of ω . However, the magnitude of phase velocity is significantly low in the low frequency range $\omega \leq 10$. It is also noticed from the phase velocity profiles that the mean of energy transportation is mechanical in the low-frequency region and predominantly thermal at high-frequency zone.

The attenuation coefficient profiles of thermally insulated and isothermal boundaries are presented in Figures 4–7, respectively, on log–linear scales with respect to frequency for different values of time lags. From the Figure 4, it is observed that for a

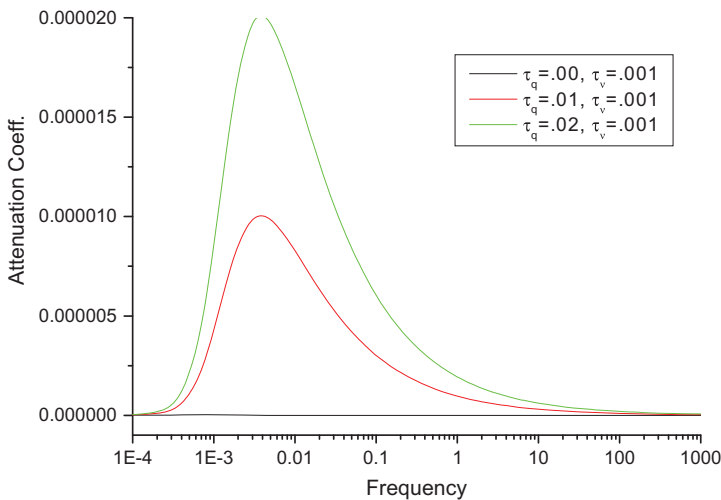


Figure 4. Variation of attenuation coefficient in insulated boundaries w.r.t. frequency (for various values of τ_q).

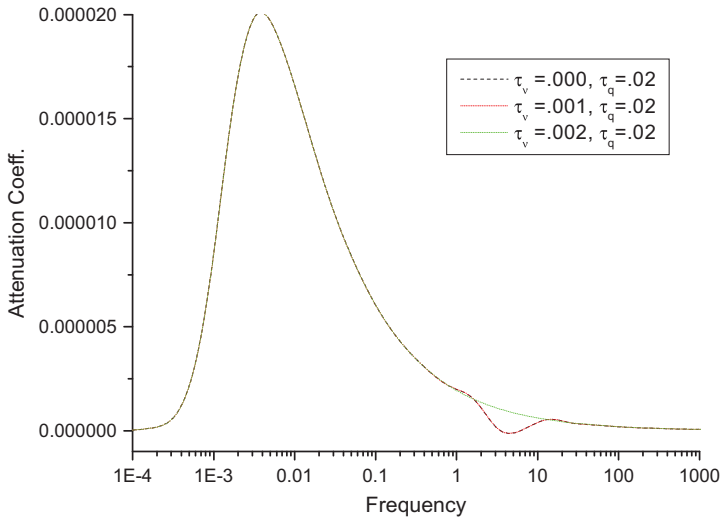


Figure 5. Variation of attenuation coefficient in insulated boundaries w.r.t. frequency (for various values of τ_v).

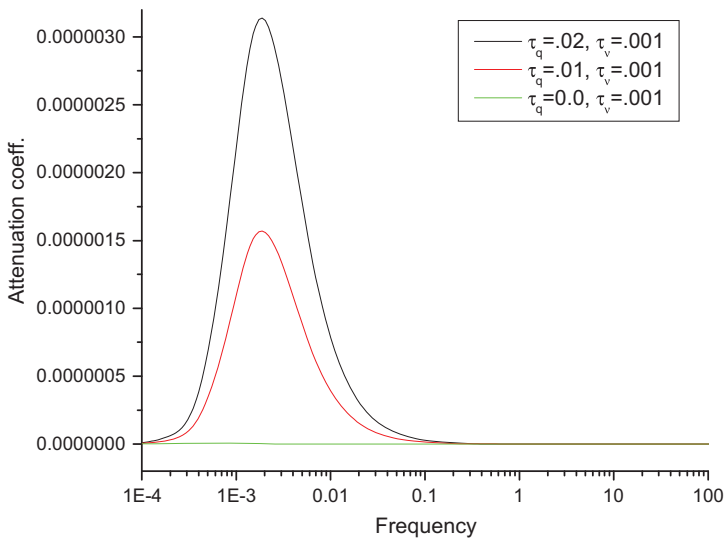


Figure 6. Variation of attenuation coefficient in isothermal boundaries w.r.t. frequency (for various values of τ_q).

fixed value of $\tau_v = .001$, attenuation coefficient increases in the frequency range $0 \leq \omega \leq .01$, decreases in the range $.01 < \omega \leq 100$ and remains constant in the range $\omega > 100$. Whereas in isothermal boundaries, attenuation coefficient increases in the range $0 \leq \omega \leq .003$, decreases in the range $.003 < \omega \leq .1$ and then remains constant. But the magnitude of the attenuation coefficients is high in insulated boundaries than that of in isothermal boundaries for same value of τ_q and τ_v .

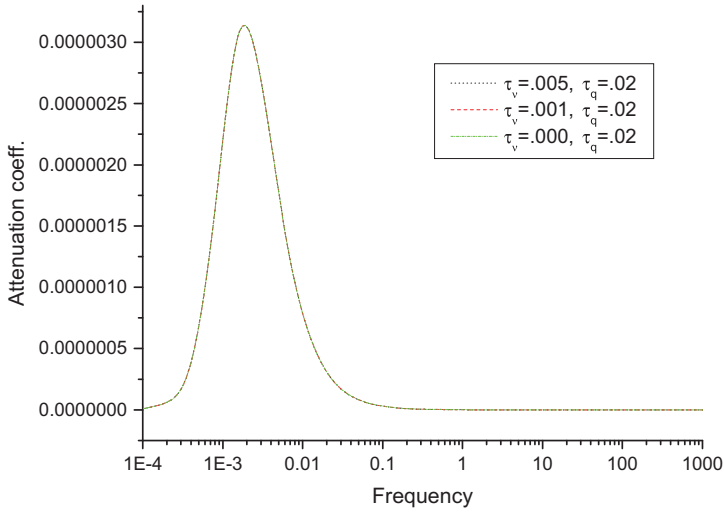


Figure 7. Variation of attenuation coefficient in isothermal boundaries w.r.t. frequency (for various values of τ_v).

Now, for fixed value of $\tau_q = .02$, when the value of τ_v is varies, the values of the attenuation coefficient are unchanged for both the boundary condition as shown in Figures 5 and 7. Therefore, in the case of attenuation coefficient, the dominating factor is the time lag due to heat flux (τ_q) over the other time lags (τ_v, τ_T).

In Figures 8–10, variations of attenuation coefficient are shown for different thermoelastic model. From Figure 8, it is noticed that in comparison with GN model, phase-lag models attain a very low values in the frequency region $.002 < \omega \leq 1000$ and then converge towards the profiles of phase-lag models. From Figures 9 and 10, it is observed that in micropolar thermoelastic half-space, attenuation coefficient takes

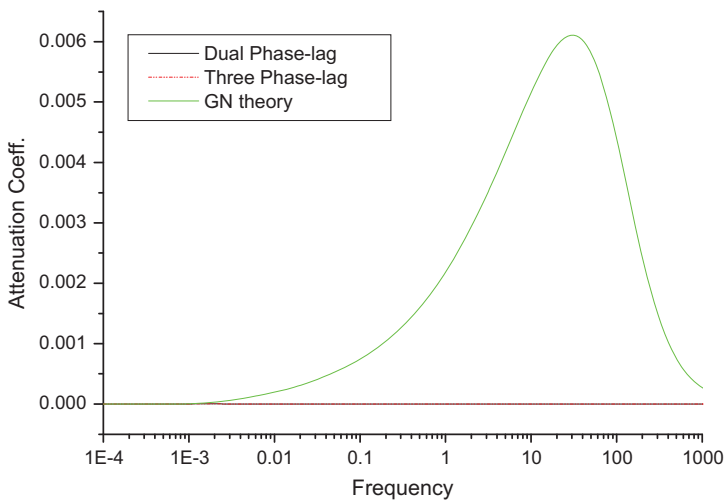


Figure 8. Comparison of attenuation coefficient in isothermal boundaries w.r.t. frequency (for different thermoelastic models).

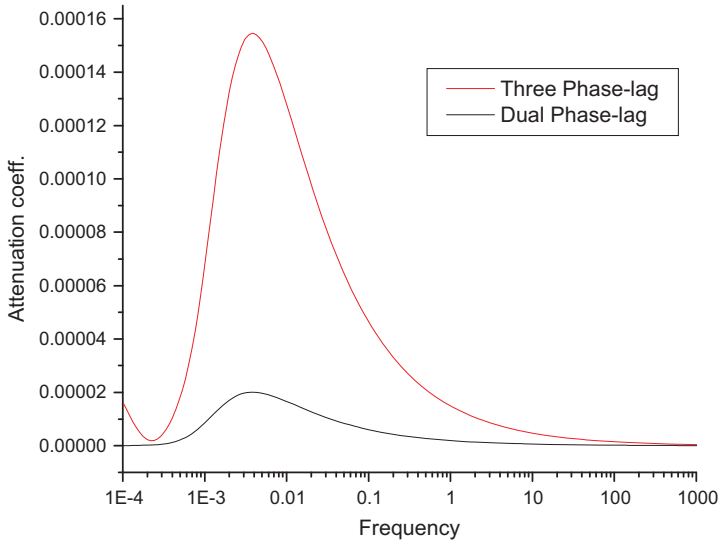


Figure 9. Variation of attenuation coefficient in insulated boundaries w.r.t. frequency (for dual and three-phase-lag models).

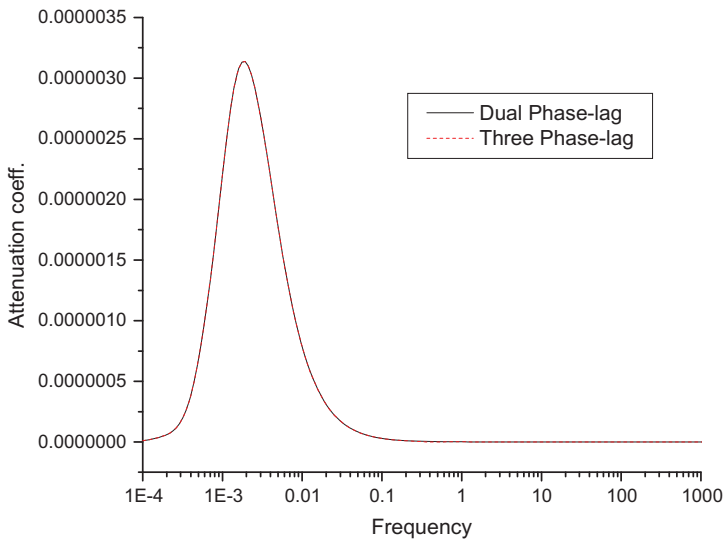


Figure 10. Comparison of attenuation coefficient in isothermal boundaries w.r.t. frequency (for dual and three-phase-lag models).

significantly small values in dual-phase-lag model with respect to three-phase-lag thermoelasticity in the case of insulated boundaries but they attain almost identical values in isothermal boundary condition. In the low frequency range, both the phase-lag models take some larger values and then converge towards zero.

From the Figures 11 and 12, it is noticed that the specific loss factor is different for different thermoelastic models and it attains a quite large value as compared with phase-lag models. Both the phase-lag models attain almost identical values as shown in Figure 12.

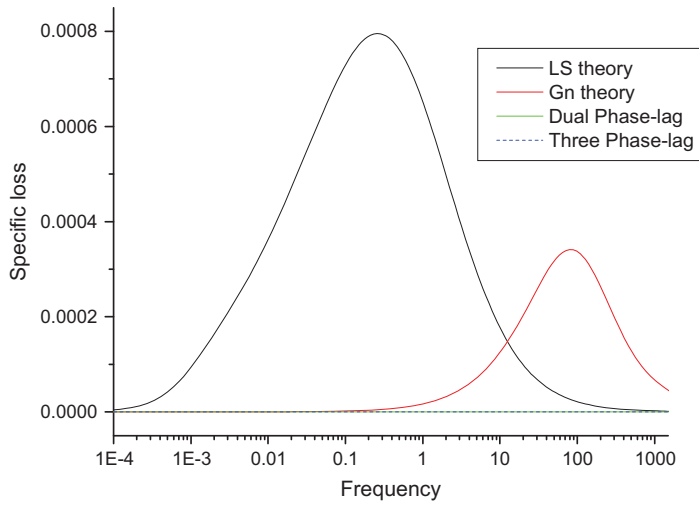


Figure 11. Variation of specific loss w.r.t. frequency (for various thermoelastic models).

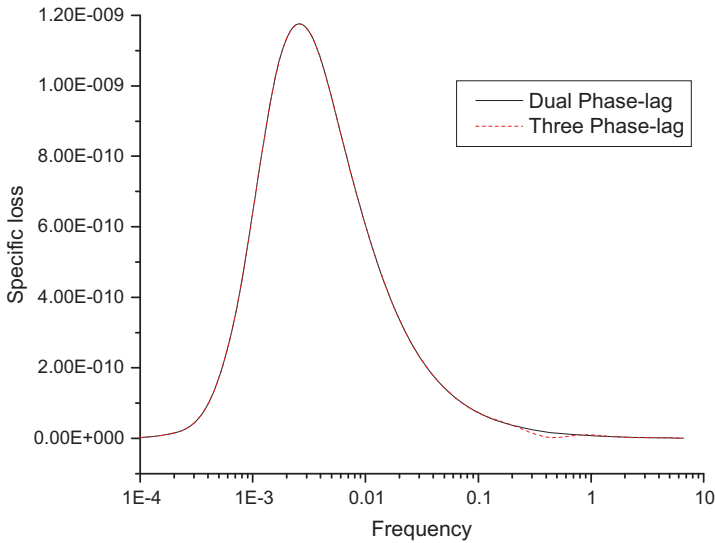


Figure 12. Comparison of specific loss w.r.t. frequency (for dual and three-phase-lag models).

9. Conclusions

The propagation of Rayleigh surface waves in a thermoelastic micropolar solid subject to thermally insulated or isothermal boundaries is investigated in the context of three-phase-lag thermoelastic model. After analytical discussions and numerical observations, we can conclude the following phenomena:

- (1) For Rayleigh surface wave propagating in a thermoelastic micropolar solid, the phase velocity remains unchanged for all the thermoelasticity models. It increases with increasing value of frequency.
- (2) Time lag due to heat flux is much dominating factor in comparison with other time lags.
- (3) For all the thermoelastic models, attenuation coefficient attains a high value in the low frequency range.
- (4) The mean energy transportation is mechanical in the low-frequency region and predominantly thermal at high frequency range.

Disclosure statement

No potential conflict of interest was reported by the authors.

References

- Abouelregal, A. E. (2011). Rayleigh waves in a thermoelastic solid half space using dual-phase-lag model. *International Journal of Engineering Science*, *49*, 781–791.
- Bai, C., & Lavine, A. S. (1992). Non-equilibrium hyperbolic type heat conduction equation. *ASME HTD*, *200*, 87–92.
- Boschi, E., & Ieşan, D. (1973). A generalized theory of linear micropolar thermoelasticity. *Meccanica*, *8*, 154–157.
- Cattaneo, C. (1948). Sulla conduzionedelcalore. *AttiSeminaro Mat. Fis. Univer. Modena*, *3*, 83–124.
- Coleman, B. D., Fabrizio, M., & Owen, D. R. (1982). On the thermodynamics of second sound in dielectric crystals. *Archive for Rational Mechanics and Analysis*, *80*, 135–185.
- Coleman, B. D., Fabrizio, M., & Owen, D. R. (1986). Thermodynamics and the constitutive relations for second sound in crystals. In J. Serrin (Ed.), *New perspectives in thermodynamics* (pp. 171–185). Berlin, Heidelberg: Springer-Verlag.
- Dhaliwal, R. S., & Singh, A. (1980). *Dynamical coupled thermoelasticity*. Delhi: Hindustan Publishers.
- Dost, S., & Tabarrok, B. (1978). Generalized micropolar thermoelasticity. *International Journal of Engineering Science*, *16*, 173–183.
- Eringen, A. C. (1966). Linear theory of micropolar elasticity. *Journal of Mathematics and Mechanics*, *15*, 909–923.
- Eringen, A. C. (1967). Mechanics of micromorphic continua. In E. Kroner (Ed.), *Mechanics of generalized continua* (pp. 18–35). Stuttgart: IUTAM Symposium Frenndensstadt.
- Eringen, A. C. (1984). Plane waves in nonlocal micropolar elasticity. *International Journal of Engineering Science*, *22*, 1113–1121.
- Eringen, A. C. (1999). *Microcontinuum field theories, foundations and solids*. New York, NY: Springer-Verlag.
- Eringen, A. C. (1964). Mechanics of micromorphic materials. In M. Gortler (Ed.), *Proceedings of the eleventh International Congress of Applied Mechanics* (pp. 131–138). New York: Springer-Verlag.
- Eringen, A. C., & Kafadar, C. B. (1976). Polar field theories. In A. C. Eringen, (Ed.), *Continuum physics 4*, 1–75. New York, NY: Academic Press.
- Eringen, A. C. (1971). Micropolar elastic solids with stretch. In I. A. Mustafa (Ed.), *24*, 1–18. Istanbul: Ari Kitabevi Matbaasi.
- Eringen, A. C., & Suhubi, E. S. (1964). Nonlinear theory of simple microelastic solids. *International Journal of Engineering Science*, *2*, 389–404.
- Green, A. E., & Lindsay, K. A. (1972). Thermoelasticity. *Journal of Elasticity*, *2*, 1–7.
- Green, A. E., & Naghdi, P. M. (1991). A re-examination of the basic postulates of thermomechanics. *Proceedings of the Royal Society A: Mathematical, Physical and Engineering Sciences*, *432*, 171–194.

- Green, A. E., & Naghdi, P. M. (1992). On undamped heat waves in an elastic solid. *Journal of Thermal Stresses*, 15, 253–264.
- Green, A. E., & Naghdi, P. M. (1993). Thermoelasticity without energy dissipation. *Journal of Elasticity*, 31, 189–208.
- Kanoria, M., & Mallik, S. H. (2010). Generalized thermoviscoelastic interaction due to periodically varying heat source with three-phase-lag effect. *European Journal of Mechanics – A/Solids*, 29, 695–703.
- Kolsky, H. (1963). *Stress waves in solids*. New York, NY: Dover Press.
- Lord, H. W., & Shulman, Y. (1967). A generalized dynamical theory of thermoelasticity. *Journal of the Mechanics and Physics of Solids*, 15, 299–309.
- Mukhopadhyay, S., & Kumar, R. (2010). Analysis of phase-lag effects on wave propagation in a thick plate under axisymmetric temperature distribution. *Acta Mechanica*, 210, 331–344.
- Puri, P., & Cowin, S. C. (1985). Plane waves in linear elastic materials with voids. *Journal of Elasticity*, 15, 167–183.
- Quintanilla, R. (2009). A well-posed problem for the three-dual-phase-lag heat conduction. *Journal of Thermal Stresses*, 32, 1270–1278.
- Quintanilla, R. (2011). Some solutions for a family of exact phase-lag heat conduction problems. *Mechanics Research Communications*, 38, 355–360.
- Quintanilla, R., & Racke, R. (2008). A note on stability in three-phase-lag heat conduction. *International Journal of Heat and Mass Transfer*, 51, 24–29.
- Roy Choudhuri, S. K. (2007a). On a thermoelastic three-phase-lag model. *Journal of Thermal Stresses*, 30, 231–238.
- Roy Choudhuri, S. K. (2007b). One dimensional thermoelastic waves in elastic half-space with dual-phase-lag effects. *Journal of Mechanics of Materials and Structures*, 2, 489–502.
- Tzou, D. Y. (1995a). A unified field approach for heat conduction from macro- to micro-scales. *Journal of Heat Transfer*, 117, 8–16.
- Tzou, D. Y. (1995b). Experimental support for the lagging behavior in heat propagation. *Journal of Thermophysics and Heat Transfer*, 9, 686–693.
- Tzou, D. Y. (1995c). The generalized lagging response in small-scale and high-rate heating. *International Journal of Heat and Mass Transfer*, 38, 3231–3240.
- Tzou, D. Y. (1997). *Macro to micro-scale heat transfer: The lagging behavior*. Washington, DC: Taylor and Francis.